Environmental Science & Technology

Article

pubs.acs.org/est

Impacts of Combustion Conditions and Photochemical Processing on the Light Absorption of Biomass Combustion Aerosol

J. Martinsson,[*,†,‡] A. C. Eriksson,[†,§] I. Elbæk Nielsen,[∥] V. Berg Malmborg,[§] E. Ahlberg,[†,‡] C. Andersen,[§] R. Lindgren,[⊥] R. Nyström,[⊥] E. Z. Nordin,[§] W. H. Brune,[#] B. Svenningsson,[†] E. Swietlicki,[†] C. Boman,[⊥] and J. H. Pagels[§]

[†]Division of Nuclear Physics, Lund University, Box 118, Lund SE-22100, Sweden

[‡]Centre for Environmental and Climate Research, Lund University, Ecology Building, Lund SE-223 62, Sweden

[§]Ergonomics and Aerosol Technology, Lund University, Box 118, Lund SE-22100, Sweden

[∥]Department of Environmental Science, Aarhus University, Roskilde 4000, Denmark

[⊥]Thermochemical Energy Conversion Laboratory, Umeå University, Umeå SE-90187, Sweden

[#]Department of Meteorology, Pennsylvania State University, University Park, Pennsylvania 16802-5013, United States

Supporting Information

ABSTRACT: The aim was to identify relationships between combustion conditions, particle characteristics, and optical properties of fresh and photochemically processed emissions from biomass combustion. The combustion conditions included nominal and high burn rate operation and individual combustion phases from a conventional wood stove. Low temperature pyrolysis upon fuel addition resulted in "tar-ball" type particles dominated by organic aerosol with an absorption Ångström exponent (AAE) of 2.5−2.7 and estimated Brown Carbon contributions of 50−70% to absorption at the climate relevant aethalometer-wavelength (520 nm). High temperature combustion during the intermediate (flaming) phase was dominated by soot agglomerates with AAE 1.0−1.2 and 85−100% of absorption at 520 nm attributed to Black Carbon. Intense photochemical processing of high burn rate flaming combustion emissions in an oxidation flow reactor led to strong formation of Secondary Organic Aerosol, with no or weak absorption. PM1 mass emission factors (mg/kg) of fresh emissions were about an order of magnitude higher for low temperature pyrolysis compared to high temperature combustion. However, emission factors describing the absorption cross section emitted per kg of fuel consumed (m^2/kg) were of similar magnitude at 520 nm for the diverse combustion conditions investigated in this study. These results provide a link between biomass combustion conditions, emitted particle types, and their optical properties in fresh and processed plumes which can be of value for source apportionment and balanced mitigation of biomass combustion emissions from a climate and health perspective.

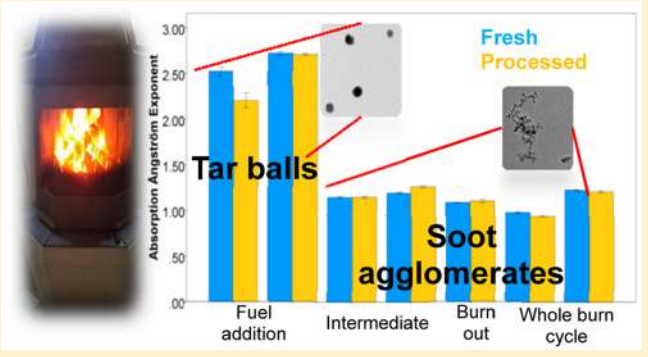

INTRODUCTION

Biomass combustion for heat and power generation is likely to increase as it is considered renewable and CO_2-neutral source. In Europe, energy consumption of solid biomass is increasing with 3.5% per year.[1] Inhalation of biomass combustion emissions have been related to adverse health effects on humans.[2−5] It has been suggested that some of the health effects are associated with the organic aerosol (OA) content, including polycyclic aromatic hydrocarbons (PAH).[6] PAHs can be emitted during ignition and intense combustion in conventional wood stoves.[7−9]

The OA has effects on the radiative balance of the earth by absorbing and scattering incoming solar radiation. It has been shown that OA can be highly light absorbing in the UV-region,[10,11] this absorbing fraction of OA is referred to as brown carbon (BrC).[10,12,13] Global model simulations have shown that BrC contributed to 19−40% of the total absorption by atmospheric aerosols.[14,15] Climate effects of OA are presently associated with large uncertainty.[16] In order to perform accurate predictions regarding the climate implications of OA and BrC, there is a need for emission factors to predict the impacts of light absorption from these groups of compounds.

Biomass combustion is a heterogeneous process. Emission levels and particle properties vary drastically among different combustion technologies. Even for a single system, the

Received: July 2, 2015
Revised: November 9, 2015
Accepted: November 12, 2015
Published: November 12, 2015

DOI: 10.1021/acs.est.5b03205
Environ. Sci. Technol. 2015, 49, 14663−14671

properties vary significantly between different burn phases. Many combustion systems are poorly controlled and large variations may also occur due to user behavior. Thus, it is a major challenge to represent these emissions in models needed to assess climate and health effects. Bølling et al.[2] represented biomass combustion emissions with three different particle types; soot agglomerates, spherical organic dominated tar-balls, and inorganic ash particles. Recent reports have found both soot agglomerates coated with organics and tar-balls in ambient air from residential wood combustion and forest fires.[17,18] These particle types may have different optical properties due to differences in both chemistry and microphysical properties.

Measurements of the wavelength dependence, i.e., the absorption Ångström exponent (AAE), of the absorption coefficient are commonly used for source apportionment of ambient PM. Traffic is commonly assumed to have AAE = 1 and biomass combustion a constant AAE = 2. Liu et al.[19] stated that more research is needed on variability of AAE from biomass combustion sources. They represented solid fuel combustion contributions to urban background air in London by two different sources that may reflect different types of biomass combustion.

Biomass combustion has been found to be a major source of BrC.[11,17,20,21] However, the relationship between biomass combustion conditions, particle types, and BrC emissions remain poorly understood. Combustion conditions, such as temperature and oxygen availability, may control the emissions of UV-absorbing OA from solid fuel combustion. For example, increasing pyrolysis temperature causes increasing brownness of the organic aerosol.[20,22] Recent studies showed that the light absorption of OA from biomass combustion increased with increasing black carbon (BC)-to-OA ratio.[21,23] The components responsible for BrC absorption are largely unknown. However, functionalized PAHs and nitrated phenols have been suggested as contributors to primary and secondary BrC, respectively.[20,24] Extremely low volatile organic compounds (ELVOCs) have also been proposed as major contributors to BrC from biomass burning.[21] These ELVOCs were suggested to be large organic molecules that are formed during low O_2-concentration and are highly UV-absorbing.[21]

The optical properties of BrC may change due to atmospheric aging.[10] Zhong and Jang[25] indicated that light absorption of biomass burning OA could both increase and decrease due to chromophore formation and sunlight bleaching (photobleaching), respectively. Saleh et al.[26] showed that both biomass primary organic aerosols (POA) and secondary organic aerosols (SOA) are absorbing. Lambe et al.[27] found only weak absorption of SOA generated from biomass burning surrogates, the absorption increased with increased oxidation level. Previous studies on effects of atmospheric aging on the optical properties of biomass combustion has been carried out in smog chambers and typically been limited to OH-exposures $<5 \times 10^7$ molecules/cm^3·h. These straggling results indicate a demand for more studies to investigate how the optical properties depend on both combustion conditions and atmospheric processing.

We have combined measurements of the optical properties and chemical composition of biomass combustion emissions with the aim to investigate the relationship between BrC and OA emissions, burn rates, and combustion phase in a conventional wood stove. The emissions were photochemically processed in a flow tube reactor which allowed studies of more intense aging than in previous smog chamber studies. The aim was to study the effects of intense atmospheric aging on chemical and optical properties of wood smoke particles. Finally, we calculated emission factors for light absorbing fractions of particulate matter (PM) with the aim that these can be applied to estimate direct climate forcing.

MATERIALS AND METHODS

Combustion Facilities and Experimental Setup. Logs of birch were combusted in a typical natural-draft conventional wood stove with a nominal heat output of 9 kW. The inside of the stove is lined with 25-mm thick soapstones. The stove is a commonly installed stove in Sweden, which very well represents the Scandinavian market during the 1990s. A detailed technical description of the wood stove and emission characterization is reported elsewhere.[7,9] A flue-gas fan regulated the flue-gas flow to improve repeatability of experiments, while maintaining relevant chimney draft of 10−15 Pa. The wood stove was operated in two modes; nominal burn rate (NB) and high burn rate (HB). NB was the condition that was adopted if the user of the stove followed the recommendation for combustion by the manufacturer, HB was created by overloading (without exceeding the likely authentic range) the stove with dry logs. More specifically, NB was achieved by combustion of 2.5 kg fuel (3 wood logs, moisture content 15%) at each batch, compared to 3.5 kg/batch (9 wood logs, moisture content 7%) for HB.

Phase division of the combustion cycles was adopted from Eriksson et al.[7] A combustion cycle is initiated with a short "fuel addition phase" (∼2 min), where the stove hatch was briefly opened and logs were added to a bed of embers. The logs then caught fire and flaming combustion occurred, this phase was defined as the "intermediate phase". The "burn out phase" started when a majority of the fuel was combusted and the excess O_2 in flue-gases reached >14%. CO, O_2, NO_x and total hydrocarbon (THC) measurements in the flue-gas corresponding to each steady state experiment in the 15 m^3 chamber is described and shown in the Supporting Information (SI, Table S1).

Aerosol Sampling. Aerosol was sampled from the flue-gas channel of the stove. A schematic of the setup is shown in Figure S1. The aerosol flow was diluted in several steps with ejector dilutors (Dekati, Finland) and time-resolved aerosol sampling was carried out to follow the dynamics of individual burn cycles. A 15 m^3 aluminum mixing chamber was included in the setup for extended sampling of aerosols from well-defined combustion conditions. For this case, aerosol from selected burn phases or complete cycles (in total 7 experiments) was further diluted and transferred to the chamber and maintained at atmospherically relevant particle concentrations (10−50 μg/m^3). Differences in stove operation during the two fuel addition experiments are described in detail in the SI. Number size distributions were measured from the mixing chamber on diluted biomass combustion aerosol with a scanning mobility particle sizer (SMPS, TSI DMA 3071, CPC 3010).

A potential aerosol mass reactor (PAM)[28,29] was connected between the mixing chamber and the instruments to study the effects of intense atmospheric processing. The PAM is a 13.5 l flow tube that utilizes UV-lamps with peak wavelengths at 185 and 254 nm to produce ozone and hydroxyl radicals (OH) that oxidizes the incoming aerosol. We estimated the OH-exposure to be 3×10^8 molecules/cm^3·h based on laboratory calibrations of SO_2 oxidation in the absence of wood smoke. This

DOI: 10.1021/acs.est.5b03205
Environ. Sci. Technol. 2015, 49, 14663−14671

corresponds to several days of atmospheric aging. However, as recently pointed out by Li et al.,[30] this is an upper estimate as the OH-reactivity (OHR) of the incoming aerosol may reduce the OH-exposure even at moderate concentrations used in this study. The total external OHR was not measured directly in this study but is estimated to range from 3 to 92 s^{-1} (see Table S1 for further details) and is not believed to suppress OH enough to reduce SOA production significantly, since the cases with highest OHR also had the highest OA enhancement (OA_{enh}). Excluding the HB experiments, the OHR was 3−21 s^{-1}, which is typical ambient OHR in urban and rural background.[30] Bruns et al.[31] recently compared mass spectra of biomass combustion aerosols upon aging in a smog chamber and the PAM at overlapping OH-exposures, they concluded that the PAM is a satisfactory model of atmospheric processing of such aerosols.

Comparison of fresh vs processed aerosol was performed by alternating the aerosol flow between the PAM and a bypass flow every 12 min. It should be pointed out that a fraction of the SOA formed in the PAM forms new smaller particles via nucleation. A fraction of the nucleated particles may appear in particles smaller than 50−70 nm, where the collection efficiency of the aerosol mass spectrometer (AMS) is reduced. Thus, the processed OA mass concentrations reported in this paper can be considered a lower limit estimate of the SOA formation.

Optical Measurements and Quantification of BrC. The light absorption of aerosols was measured with a seven wavelength (370, 470, 520, 590, 660, 880, 950 nm) aethalometer (AE33, Magee Scientific)[32] operated with a flow rate of 2 L per minute. The aethalometer utilizes an airflow through a filter where particles are deposited. Seven LEDs irradiate the filter, and a photodetector measures the attenuation through the filter which increases with increased particle deposition. Two recognized measurement artifacts are common in filter-based absorption measurements, i.e., filter matrix light scattering and the filter loading effect.[33] Enhancement of absorption due to filter matrix scattering is compensated automatically in the AE33 by a factor of 1.57, and the filter loading effect is treated by measuring the attenuation at two aerosol deposition spots with different deposition rates.[32]

BC is highly absorbing in the visible spectrum. The absorption is considered to vary relatively weakly with wavelength and shows an AAE around 1.0.[34] As BrC is highly light absorbing in the UV-range, BrC containing emissions exhibit an AAE above 1. On the basis of Sandradewi et al.,[35] we used a simple model to separate the total measured light absorbing carbon (LAC) at each wavelength (λ) into BrC and BC. LAC_λ is thus defined as follows:

$$LAC_\lambda = BC_\lambda + BrC_\lambda \tag{1}$$

The BC absorption (BC_λ) was calculated by assuming that all light absorption in 880 and 950 nm was solely due to BC.[11,36] An average of the light absorption in 950 and 880 nm was calculated and then extrapolated with $AAE_{BC} = 1$ to calculate BC_λ for the other wavelengths (370−660 nm):

$$BC_\lambda = \left(\frac{LAC_{950nm} + LAC_{880nm}}{2}\right) \times \left(\frac{\lambda}{\left(\frac{950+880}{2}\right)}\right)^{-AAE_{BC}} \tag{2}$$

$$AAE = \frac{\log \frac{LAC_{\lambda 1}}{LAC_{\lambda 2}}}{\log \frac{\lambda_1}{\lambda_2}} \tag{3}$$

Chemical Characterization. Highly time-resolved chemical quantification of the combustion aerosols were performed in situ with a soot-particle aerosol mass spectrometer (SP-AMS).[37] Aerosol is sampled into a vacuum system connected to a mass spectrometer to allow highly time-resolved in situ measurements. Two alternating aerosol vaporization modes are used; flash vaporization on a 600 °C tungsten plate, and the dual vaporization mode, adding laser vaporization using a 1064 nm continuous Nd:YAG intracavity laser. The laser enables detection of refractory species which absorb IR radiation, such as BC. The vapors are then ionized using 70 eV electron ionization and separated by mass-to-charge ratio with time-of-flight mass spectrometry. We here present the total organic PM (OA) and rBC (refractory black carbon measured by SP-AMS).[37] A description of the sensitivity and calibration of the SP-AMS can be found in the SI.

Absorption Emission Factors. For this kind of biomass combustion system, the emission factors are usually expressed in emitted PM mass per generated unit of energy (e.g., mg/MJ) or per kg of fuel consumed. In this study, we determined light absorption, thus EF_{abs} is expressed in m^2/MJ and m^2/kg according to eqs 4 and 5. EF_{abs} represents the absorption cross section emitted to the atmosphere per MJ generated or per kg of fuel consumed.

$$EF_{abs\_MJ}\left[\frac{m^2}{MJ}\right] = \frac{FGV\left[\frac{m^3}{kg}\right]}{HV_{fuel}\left[\frac{MJ}{kg}\right]} \times b_{abs}[m^{-1}] \tag{4}$$

$$EF_{abs\_kg}\left[\frac{m^2}{kg}\right] = FGV\left[\frac{m^3}{kg}\right] \times b_{abs}[m^{-1}] \tag{5}$$

In eqs 4 and 5, the absorption coefficient (b_{abs}) is measured in m^{-1} for LAC, which can be separated into absorption coefficients for BrC and BC according to eqs 1 and 2. To get the light absorption emission factor in m^2/MJ, we multiply the measured absorption coefficients with the flue-gas volume (FGV) and divide by the heating value of the wood logs (HV_{fuel}, 19 MJ/kg).[9] The FGV is the volume of flue-gas at standard temperature and pressure and dry conditions resulting from combustion of 1 kg wood fuel. FGV is calculated using a simple mass balance model, which assumes complete combustion.[38] FGV increases with increasing O_2 mixing ratio in the undiluted flue-gas. By removing the HV_{fuel} parameter from eq 4, absorption emission factors in the unit m^2/kg can also be obtained.

RESULTS AND DISCUSSION

Absorption Ångström Exponents. In Figure 1, AAE and transient emissions are presented for a typical combustion batch carried out at nominal burn rate (NB). A batch of wood logs is added on glowing embers at t = 0, leading to low temperature pyrolysis as volatile organics (and water) are volatilized. This results in high organic aerosol emissions with a high AAE of about 2. The intermediate phase starts when flames occur and the O_2 in the flue-gas drops below 14%. At the beginning of this phase, the heat release rate from the fuel increases, and the combustion temperature increases strongly.

DOI: 10.1021/acs.est.5b03205
Environ. Sci. Technol. 2015, 49, 14663−14671

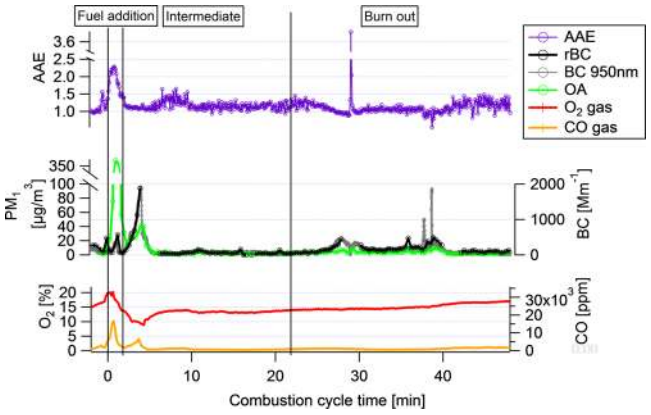

Figure 1. Transient emissions and optical properties during a typical full NB cycle (three wood logs were added at t = 0). Time-resolved AAE as measured with the aethalometer (upper panel). Diluted (200 times) organic aerosol (OA), rBC, and total light absorption coefficient at 950 nm (BC) (middle panel). O_2 (red) and CO (orange) concentration in the flue-gas (lower panel). The main features of the cycle are reproducible.

This results in a decrease in AAE to values of 1.0−1.4. During the intermediate phase, BC is dominating over OA, and the emissions are generally low, except for a brief period just after the flames first appeared. In the final burn out phase which starts as the O_2 in the flue-gas increases above 14%, the fraction of the fuel undergoing flaming combustion is small. Generally, the AAE is between 0.9 and 1.3, with a very short-lived peak at 28 min (Figure 1). This peak is hard to explain, as it did not occur in most batches. There are also some emission peaks in BC at 37 min.

In Figure 2, the AAE is summarized for seven experiments with emissions from individual combustion phases or full cycles. The given emissions were diluted and transferred to the 15 m^3 steel chamber and sampling was carried out from this

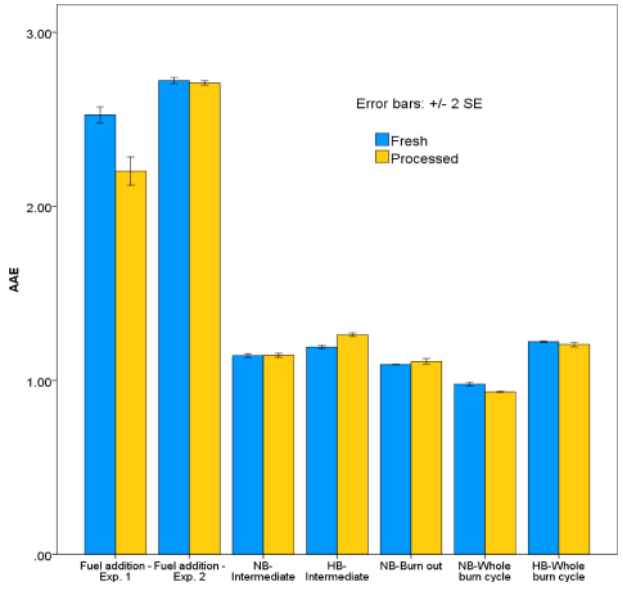

Figure 2. Absorption Ångström Exponent (AAE, 370−950 nm) for different phases during a burn cycle. Blue bars represent the fresh unprocessed aerosol, while orange bars represents photochemically processed aerosol with the PAM flow tube. The error bars represent ±2 standard errors (SE) over time.

chamber at stationary conditions either through the PAM flow reactor (processed emissions) or in the bypassed mode (fresh emissions). The fuel addition experiments exhibit AAE ranging from 2.5 to 2.7. TEM images showed spherical tar-ball-like particles for these cases (Figure S5). In fuel addition, experiment #1, the AAE dropped from 2.5 to 2.2 upon aging by UV-exposure in the PAM oxidation flow reactor. Experiments with the intermediate phase, burn out phase, and whole burn cycle all showed an AAE of 1.0−1.2. TEM images showed fractal-like soot agglomerates with primary particle diameters 25−35 nm for these cases (Figure S6). The AAE was slightly higher for high burn rate (HB) compared to nominal burn rate (NB) for both whole burn cycles and for the intermediate phase. Only weak changes in AAE were observed during photochemical processing, in these experiments.

Saleh et al.[26] reported AAE from combustion of three wood species with the aim to simulate wild-fires. They found AAE ranging from 1.35 to 2.15 for the unprocessed aerosols and slightly higher values upon smog chamber processing. Kirschtetter et al.[11] found AAE = 2.5 for fire wood samples and samples from savannah fires. Most literature data are within the range of our data (AAE = 1.0−2.7). Thus, our data may cover both ends of the complex spectrum of biomass combustion conditions being: 1. Low temperature pyrolysis which in our study came from the first few minutes after adding new wood logs, but may also occur during smoldering combustion in outdoor burning of humid fuels. 2. BC dominated aerosol from flaming high temperature combustion in well insulated wood stoves.

Effect of Combustion Conditions and Burn Cycle Phases on Optical Properties. LAC separation into BC and BrC according to eqs 1−3 was applied to the experiments where emissions from selected combustion phases were transferred to the 15 m^3 steel chamber. Figure 3 shows two examples of time-series to illustrate the large difference in BC and BrC fractions between experiments. The mean aerosol mass concentration in the chamber was approximately 50 $\mu g/m^3$ and had a residence time of at least 30 min in order to stabilize before sampling. Sampling from the chamber was alternated either bypass or through the PAM (OH-exposure ~3 × 10^8 molecules/cm^3·h).

Emissions from the fuel addition phase (low temperature pyrolysis) were dominated by OA, and BrC dominated over BC (Figure 3A). Processing in the PAM led to no net production of OA in this experiment. The BrC absorption decreased about 30% indicating photobleaching of the OA upon aging. Photobleaching has previously been demonstrated in smog chamber experiments.[25] The rBC signal from the SP-AMS increased by almost 50% upon processing. It is not clear why, but the collection efficiency of the SP-AMS may change upon processing and depends on many factors including particle morphology.[39]

Emissions from the intermediate flaming phase in a high burn rate experiment (high temperature air-starved combustion) were dominated by BC absorption (Figure 3B). It showed extensive SOA formation, with OA_{enh} of about a factor of 10 (i.e., the organic mass concentration was ten times higher when sampling through the PAM, compared with bypass). However, the SOA formation had essentially no effect on the measured optical properties. The BC (and rBC) concentrations were marginally affected, suggesting that particle losses in the PAM were less than 10% by mass.

DOI: 10.1021/acs.est.5b03205
Environ. Sci. Technol. 2015, 49, 14663−14671

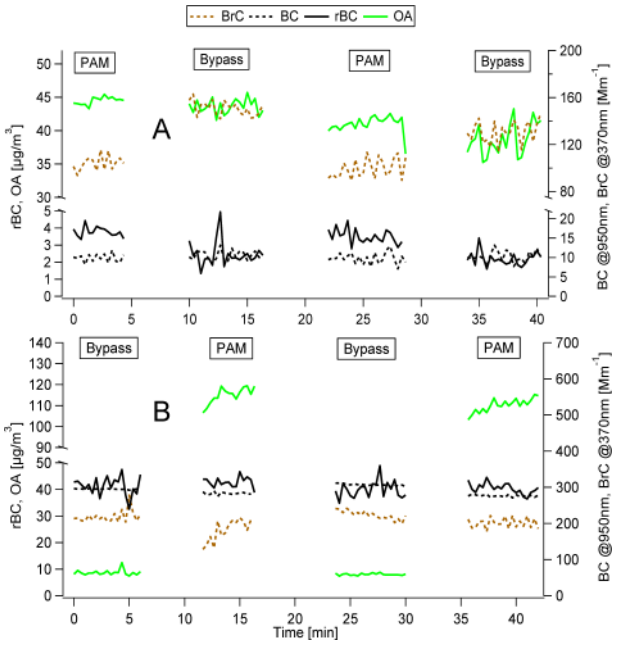

Figure 3. Time-series illustrating the effects of photochemical processing with the PAM flow tube on organic aerosol concentrations and optical properties. Diluted aerosol from well-defined combustion phases was transferred to the 15 m^3 steel chamber before sampling commenced. (A) Low temperature combustion/pyrolysis during the fuel addition phase (Exp: fuel addition #1) illustrating BrC dominated aerosol that becomes partly bleached upon aging. Aging had little effect on the OA concentration in this experiment, (B) high burn rate emissions from the intermediate phase (Exp: HB-Intermediate) are dominated by BC. The data show evidence of strong SOA formation of essentially non-light absorbing material.

The ratio between BrC and LAC for different combustion conditions (NB, HB) and combustion phases are illustrated in Figure 4. BrC dominated the LAC emissions for the shorter wavelengths during the fuel addition phase experiments and accounted for 20−75% of the total absorption. As expected, the

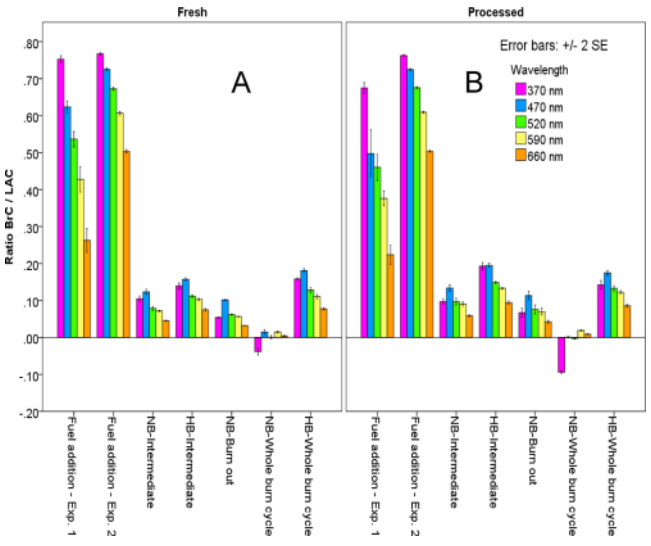

Figure 4. Estimated BrC-to-LAC ratio using the simple model for different combustion phases and burn cycles. (A) Fresh aerosol. (B) Photochemical processed aerosol. An AAE_{BC} of 1.0 was assumed. The error bars represent ±2 SE over time.

highest fraction of BrC was observed for UV-absorption (370 nm) and the contribution of BrC to LAC decreased with increasing wavelength. Since the solar intensity wavelength maxima are close to 520 nm, this channel can be regarded as the most climate-relevant. At this wavelength, BrC emissions accounted for 45−65% of LAC in the fuel addition phase experiments. A slight decrease in the BrC-to-LAC ratio upon processing was found in fuel addition phase experiment #1 due to photobleaching (Figure 4B). During the intermediate phase, burn out phase, and for the whole burn cycles, the LAC was dominated by BC (80−95%). The BrC fraction was higher for HB compared to NB both for full cycles and for the intermediate phase, although much smaller than that for the fuel addition phase. Photochemical processing of the emissions had limited effect on the wavelength dependency of BrC.

Relationship between Combustion Conditions, Chemical Composition, Processing, and the Optical Properties. We used SP-AMS data to link aerosol chemical composition with the observed optical properties. Figure 5

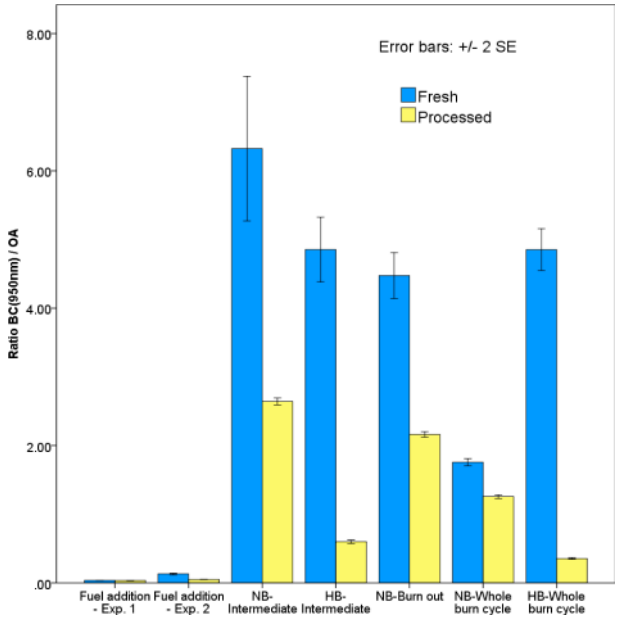

Figure 5. BC-to-OA mass-ratio for different phases during a burn cycle. Blue bars represent the fresh unprocessed aerosol, while yellow bars represent photochemically processed aerosol. BC is measured by the aethalometer at 950 nm and transformed to mass concentration using the manufacturer mass absorption coefficient (MAC) at 950 nm (7.19 m^2/g). The error bars represent ±2 SE over time.

presents the BC-to-OA mass-ratio for the different combustion conditions and phases. The fuel addition experiments gave a significantly lower BC-to-OA mass-ratio (factor 20 on average) than other combustion phases. It is expected, as low temperature pyrolysis is known to result in high emissions of OA.[7] The low temperature also means graphitization is not occurring, hence the relative absence of BC. Thus, a significant fraction of the LAC light absorption in this phase was due to OA.

A significant increase in OA was measured during photochemical processing, which lowered the BC-to-OA mass-ratio for all burn phases and burn rates, except for fuel addition experiment #1 (Figure 5). HB experiments consistently showed larger increases in OA_{enh} than that in NB and also the largest absolute SOA production. HB showed an average OA_{enh} factor

DOI: 10.1021/acs.est.5b03205
Environ. Sci. Technol. 2015, 49, 14663−14671

of 9.6, while NB showed a factor of 1.8. Thus, the OA_{enh} was 5 times higher in HB compared to NB. However, this formed SOA is not light absorbing to any significant degree.

Bruns et al.[40] aged biomass wood stove emissions photochemically in a smog chamber with an OH-exposure of 2−5 × 10^7 molecules/cm^3·h. In their experiment, the OA increased by a factor of 3 ± 1 for high fuel load experiments and 1.6 ± 0.4 for the average fuel load experiments. The larger OA_{enh} in our study compared to Bruns et al.[40] can be explained by the more intense photochemical processing used in our study, the difference in OH-exposure is an order of magnitude (2−5 × 10^7 vs 3 × 10^8 molecules/cm^3·h). Bruns et al.[40] attributed the high SOA formation for high fuel load to small PAHs (e.g., naphthalenes). Pettersson et al.[9] reported detailed gas-phase analysis of emissions from the stove type used in our study at similar conditions. On the basis of these results, known SOA yields and the high OH-exposure in our study, we find that benzene in addition to PAHs may have been an important SOA precursor. In contrast, less than 10% of benzene had reacted with OH at typical conditions in the study by Bruns et al.[40]

Lambe et al.[27] found that SOA from naphthalene showed increased absorption/brownness with increasing OH-exposure in the PAM. However, the mass absorption coefficients (MAC) were only about 1% of those of BC at 405 nm. The BC-to-OA mass-ratios in the processed HB emissions in our study were about 0.5. Thus, if the SOA was purely from naphthalene, it would have been below detection in our study.

Saleh et al.[26] found that both POA and SOA from biomass combustion absorbed light in the UV-range. The absorption of SOA was shifted toward shorter wavelengths compared to POA, thus the SOA had stronger wavelength dependence and AAE increased upon processing. We propose a few explanations for the differences between their findings and our study. Saleh et al.[26] used relatively mild aging in a smog chamber (OH-exposures up to 2.3 × 10^7 molecules/cm^3·h). Also, Saleh et al.[26] carried out experiments for BC-to-OA mass-ratios below 1 in fresh emissions. One could speculate that a majority of their particles were tar-ball types and would therefore be more similar to the fuel addition experiments in our study. We found evidence for photobleaching in fuel addition experiment #1, which showed no net increase in OA upon processing. The second experiment that had net SOA formation, OA_{enh} = 2.4, showed little effect of processing on the optical properties. It is likely that the formation of secondary BrC and photobleaching of both primary and secondary BrC depend on the OH-exposure and that competing effects (photobleaching vs formation of secondary BrC) resulted in the small effects of processing on the optical properties of fuel addition emissions found in our study.

The relatively large difference between fuel addition #1 and #2 in OA_{enh} and photobleaching can be understood from differences in combustion conditions (as described in more detail in SI). OA mass spectra of fresh and processed emissions for these two experiments are given in Figures S13 and S14. Fuel addition #1, resulting from pyrolysis at artificially reduced temperature, shows low BC-to-OA mass-ratio (0.05) and O:C ratio of 0.17, with weak signatures of levoglucosan (m/z = 60, 73) and very weak signals from methoxy phenols (for example m/z = 167). Fuel addition #2, resulting from pyrolysis at higher temperature during a default fuel addition, has a higher BC-to-OA mass-ratio (0.15) and O:C ratio (0.56) and shows distinct signatures of both levoglucosan and methoxy phenols as well as other fragments associated with aromatic structures. The higher OA_{enh} in fuel addition #2 may be associated with a larger emission of aromatics, such as methoxyphenols, that are known SOA precursors. Fuel addition #1 has a slightly higher AAE of fresh emissions (2.7 vs 2.5). However, fuel addition #2 shows a higher MAC value for the OA emissions (MAC_{OA}: 5 vs 1.1 m^2/g) at 470 nm. This is consistent with increasing MAC with increasing BC-to-OA mass-ratio[21,23] and increasing pyrolysis temperature.[20] A large range of OA_{enh} and a poor reproducibility from burn to burn has been described in literature.[41] We hypothesize that the pyrolysis temperature is not only a major determinant of the optical properties,[20] but also for the OA chemistry, OA emission factor, and SOA formation potential. Elucidating such relationships should be a primary goal of future studies.

Emission Factors of LAC. Light absorption emission factors were calculated for LAC and are presented in Figure 6.

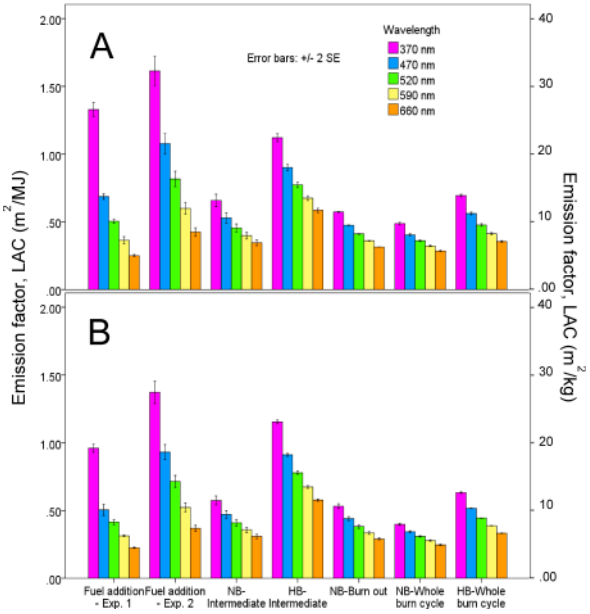

Figure 6. Emissions factors of LAC for different phases during a burn cycle. (A) Represents unprocessed aerosol and (B) represents photochemical processed aerosol. The error bars represent ±2 SE over time.

Emission factors for BC and BrC can be found in the Figure S3 and S4 . Since we measured absorption, and wood stove operation is energy related, the reported units are in m^2/MJ. Thus, the measured LAC is directly linked to the heat generation and does not include errors due to uncertainties of the MAC. Note that the unit m^2/MJ can be rescaled using the heating values into m^2/kg dry biomass in nonenergy related contexts.

There is a difference in emission of LAC with regard to combustion conditions where emissions from HB are more light absorbing per MJ of generated heat than emissions from NB. This is most likely an effect from strongly absorbing BC, which have a higher emission factor for HB than NB (Figure S3). It is also evident that the UV-absorption (370 nm) is strongest in the fuel addition phases. This strong UV-absorption gives high BrC emission factors (Figure S4). In the climate-relevant 520 nm channel, we find the highest emission factors in fuel addition experiment #2 and HB-intermediate phase. In order to limit climate forcing by LAC at local and regional scales, overloading of the stove should be

DOI: 10.1021/acs.est.5b03205
Environ. Sci. Technol. 2015, 49, 14663−14671

avoided. Avoiding stove overloading also has the benefit of reducing soot emissions and carcinogenic PAH-emissions.

The absorption emission factors are within a factor of 3 including all these vastly varying combustion conditions. In contrast, the PM1 primary emission factors vary by up to a factor of 15 between these same experiments. They were 5−11, 0.8−1.5, and 0.7−0.8 mg/kg for fuel addition, HB, and NB, respectively. Low temperature pyrolysis during fuel addition results in much higher mass emission factors compared to high temperature flaming combustion. However, these are primarily organic emissions, which typically have lower MAC than the BC-rich emissions from high temperature flaming combustion. The end-result is that the BrC-rich low temperature pyrolysis emissions and the BC-rich high temperature flaming emissions get similar optical absorption emission factors. As previously pointed out fuel addition #2 had a 4 times higher MAC_{OA} value than fuel addition #1 at 470 nm, but the OA PM1 emission factors were reverse leading to a two times higher BrC (and LAC) emission for fuel addition #2.

Implication for Source Attribution and Comparison with Field Observations. The well-used aethalometer-model to perform source apportionment calculations usually use an AAE of ∼2 for wood smoke and an AAE of ∼1 for traffic emissions.[35] However, the low AAE of 1.0−1.2 consistently found in whole burn cycles in this study suggest source apportionments efforts based on aethalometer data will misattribute emissions from well-insulated appliances such as the wood stove studied here.[9] It is possible that real-world biomass combustion plumes typically originate from a mixture of well insulated and operated stoves emitting soot agglomerate dominated aerosol (AAE ≈ 1), like the system used here, and other systems that emit tar-ball type aerosol (AAE > 2). These may add up to an average AAE of ∼2 if the emissions from these two types of systems are comparable. Additionally, aging at low OH-exposures may produce SOA with higher AAE which are in line with the findings of Saleh et al.[26] This would further explain the ambient observations.

Uncertainties Related to Internal Mixing and Assumptions of BC Absorption in Mixed Particles. Saleh et al.[26] pointed out that filter-based techniques such as the aethalometer may provide accurate measurements of AAE, but they are more vulnerable when it comes to differentiating between absorption related to OA and BC. In particular, the absorption enhancement due to internal mixing of OA with BC ("lensing") is not typically captured with the aethalometer. Saleh et al.[26] derived two limiting cases, either omitting or maximizing absorption enhancement due to internal mixing. Our analysis is similar to the case where internal mixing is ignored. For significant absorption enhancement to occur, typically the BC-to-OA mass-ratio of the individual particles would need to be smaller than about 1.[42,43] Such absorption enhancement may occur for the fuel addition but not for the remaining phases, with the exception of the high burn rate processed aerosols. Thus, even if little secondary BrC is formed under the conditions studied here, SOA formation may still induce absorption amplification due to lensing to a degree larger than what is found with the aethalometer.

This study demonstrates the controlling impact of combustion conditions on the chemical and optical properties of biomass combustion aerosols. Low temperature pyrolysis during the fuel addition phase leads to tar-ball-like particles dominated by organic matter which show high light absorption in UV/blue and AAE of around 2.5. The intermediate phase during high temperature flaming combustion led to moderately coated soot agglomerates with an AAE close to 1. For the studied wood stove AAE was close to 1 also for whole cycle emissions. The access to EFs for fractions of or a whole burn cycle can be of great value for estimations of radiative forcing over regions with high impact of wood burning in conventional stoves. Photochemical processing led to variable amounts of SOA; however, this SOA had little effect on light absorption properties measured with the aethalometer. Future studies should aim to investigate changes in optical properties of biomass combustion aerosol as a function of OH-exposure.

■ ASSOCIATED CONTENT

Supporting Information

The Supporting Information is available free of charge on the ACS Publications website at DOI: 10.1021/acs.est.5b03205.

Schematic of the experimental sampling setup, SP-AMS sensitivity and calibration, technical details regarding the PAM, differences in stove operation and OA chemical composition during the fuel addition experiments. Measured and estimated flue-gases and OHR. Also, results from the sensitivity analysis of varied AAE, TEM images, emission factors, and number-size distributions from the experiments (PDF)

■ AUTHOR INFORMATION

Corresponding Author

*Phone: +46 46 222 76 28; e-mail: johan.martinsson@nuclear.lu.se (J.M.).

Notes

The authors declare no competing financial interest.

■ ACKNOWLEDGMENTS

This study was financed by the Swedish research councils FORMAS (projects 2011-743 and 2013-1023) and VR (project 2013-5021). We acknowledge Dr. Kirsten Kling of NRCWE for excellent TEM images.

■ REFERENCES

(1) European Environmental Agency Website; http://www.eea.europa.eu/data-and-maps/indicators/renewable-primary-energy-consumption-3/assessment.

(2) Bølling, A. K.; Pagels, J.; Yttri, K. E.; Barregard, L.; Sallsten, G.; Schwarze, P. E.; Boman, C. Health effects of residential wood smoke particles: the importance of combustion conditions and physicochemical particle properties. *Part. Fibre Toxicol.* **2009**, *6* (1), 2910.1186/1743-8977-6-29.

(3) Naeher, L. P.; Brauer, M.; Lipsett, M.; Zelikoff, J. T.; Simpson, C. D.; Koenig, J. Q.; Smith, K. R. Woodsmoke Health Effects: A Review. *Inhalation Toxicol.* **2007**, *19* (1), 67−106.

(4) Sehlstedt, M.; Dove, R.; Boman, C.; Pagels, J.; Swietlicki, E.; Löndahl, J.; Westerholm, R.; Bosson, J.; Barath, S.; Behndig, A. F.; Pourazar, J.; Sandström, T.; Mudway, I. S.; Blomberg, A. Antioxidant airway responses following experimental exposure to wood smoke in man. *Part. Fibre Toxicol.* **2010**, *7* (1), 2110.1186/1743-8977-7-21.

(5) Sigsgaard, T.; Forsberg, B.; Annesi-Maesano, I.; Blomberg, A.; Bølling, A.; Boman, C.; Bønløkke, J.; Brauer, M.; Bruce, N.; Héroux, M.-E.; Hirvonen, M.-R.; Kelly, F.; Künzli, N.; Lundbäck, B.; Moshammer, H.; Noonan, C.; Pagels, J.; Sallsten, G.; Sculier, J.-P.; Brunekreef, B. Health impacts of anthropogenic biomass burning in the developed world. *Eur. Respir. J.* **2015**, ERJ-01865-2014.

(6) IARC monographs on the evaluation of carcinogenic risks to humans. *IARC Monogr. Eval. Carcinog. Risks Hum.* **2012**, *95*, 9−38.

DOI: 10.1021/acs.est.5b03205
Environ. Sci. Technol. 2015, 49, 14663−14671

(7) Eriksson, A. C.; Nordin, E. Z.; Nyström, R.; Pettersson, E.; Swietlicki, E.; Bergvall, C.; Westerholm, R.; Boman, C.; Pagels, J. H. Particulate PAH Emissions from Residential Biomass Combustion: Time-Resolved Analysis with Aerosol Mass Spectrometry. *Environ. Sci. Technol.* **2014**, *48* (12), 7143−7150.
(8) Orasche, J.; Schnelle- Kreis, J.; Schon, C.; Hartmann, H.; Ruppert, H.; Arteaga-Salas, J. M.; Zimmermann, R. Comparison of emissions from wood combustion. Part 2: impact of combustion conditions on emission factors and characteristics of particle − bound organic species and polycyclic aromatic hydrocarbon (PAH)-related toxicological potential. *Energy Fuels* **2013**, *27* (3), 1482−1491.
(9) Pettersson, E.; Boman, C.; Westerholm, R.; Boström, D.; Nordin, A. Stove Performance and Emission Characteristics in Residential Wood Log and Pellet Combustion, Part 2: Wood Stove. *Energy Fuels* **2011**, *25*, 315−323.
(10) Laskin, A.; Laskin, J.; Nizkorodov, S. A. Chemistry of Atmospheric Brown Carbon. *Chem. Rev.* **2015**, *115* (10), 4335−4382.
(11) Kirchstetter, T. W.; Novakov, T.; Hobbs, P. V. Evidence that the spectral dependence of light absorption by aerosols is affected by organic carbon. *J. Geophys. Res.* **2004**, *109* (D21), 208.
(12) Petzold, A.; Ogren, J. A.; Fiebig, M.; Laj, P.; Li, S.-M.; Baltensperger, U.; Holzer-Popp, T.; Kinne, S.; Pappalardo, G.; Sugimoto, N.; Wehrli, C.; Wiedensohler, A.; Zhang, X.-Y. Recommendations for reporting "black carbon" measurements. *Atmos. Chem. Phys.* **2013**, *13*, 8365−8379.
(13) Andreae, M. O.; Gelencsér, A. Black or brown carbon? The nature of light-absorbing carbonaceous aerosols. *Atmos. Chem. Phys.* **2006**, *6*, 3131−3148.
(14) Feng, Y.; Ramanathan, V.; Kotamarthi, V. R. Brown carbon: a significant atmospheric absorber of solar radiation? *Atmos. Chem. Phys.* **2013**, *13*, 8607−8621.
(15) Lin, G.; Penner, J. E.; Flanner, M. G.; Sillman, S.; Xu, L.; Zhou, C. Radiative forcing of organic aerosol in the atmosphere and on snow: Effects of SOA and brown carbon. *J. Geophys. Res. Atmos.* **2014**, *119*, 7453−7476.
(16) *Working group I Contribution to the IPCC Fifth Assessment Report, Climate Change 2013: The Physical Science Basis, Summary for Policymakers*, http://www.ipcc.ch/report/ar5/wg1/.
(17) Lack, D. A.; Langridge, J. M.; Bahreini, R.; Cappa, C. D.; Middlebrook, A. M.; Schwarz, J. P. Brown carbon and internal mixing in biomass burning particles. *Proc. Natl. Acad. Sci. U. S. A.* **2012**, *109* (37), 14802−14807.
(18) China, S.; Mazzoleni, C.; Gorkowski, K.; Aiken, A. C.; Dubey, M. K. Morphology and mixing state of individual freshly emitted wildfire carbonaceous particles. *Nat. Commun.* **2013**, *4*, 10.1038/ncomms3122.
(19) Liu, D.; Allan, J. D.; Young, D. E.; Coe, H.; Beddows, D.; Fleming, Z. L.; Flynn, M. J.; Gallagher, M. W.; Harrison, R. M.; Lee, J.; Prevot, A. S. H.; Taylor, J. W.; Yin, J.; Williams, P. I.; Zotter, P. Size distribution, mixing state and source apportionment of black carbon aerosol in London during wintertime. *Atmos. Chem. Phys.* **2014**, *14*, 10061−10084.
(20) Chen, Y.; Bond, T. C. Light absorption by organic carbon from wood combustion. *Atmos. Chem. Phys.* **2010**, *10*, 1773−1787.
(21) Saleh, R.; Robinson, E. S.; Tkacik, D. S.; Ahern, A. T.; Liu, S.; Aiken, A. C.; Sullivan, R. C.; Presto, A. A.; Dubey, A. K.; Yokelson, R. J.; Donahue, N. M.; Robinson, A. L. Browness of organics in aerosols from biomass burning linked to their black carbon content. *Nat. Geosci.* **2014**, *7*, 647−650.
(22) Bond, T. C. Spectral dependence of visible light absorption by carbonaceous particles emitted from coal combustion. *Geophys. Res. Lett.* **2001**, *28* (21), 4075−4078.
(23) Lu, Z.; Streets, D. G.; Winijkul, E.; Yan, F.; Chen, Y.; Bond, T. C.; Feng, Y.; Dubey, M. K.; Liu, S.; Pinto, J. P.; Carmichael, G. R. Light Absorption Properties and Radiative Effects of Primary Organic Aerosol Emissions. *Environ. Sci. Technol.* **2015**, *49*, 4868−4877.
(24) Mohr, C.; Lopez-Hilfiker, F. D.; Zotter, P.; Prévôt, A. S. H.; Xu, L.; Ng, N. L.; Herndon, S. C.; Williams, L. R.; Franklin, J. P.; Zahniser, M. S.; Worsnop, D. R.; Knighton, W. B.; Aiken, A. C.; Gorkowski, K. J.; Dubey, M. K.; Allan, J. D.; Thornton, J. A. Contribution of Nitrated Phenols to Wood Burning Brown Carbon Light Absorption in Detling, United Kingdom during Winter Time. *Environ. Sci. Technol.* **2013**, *47* (12), 6316−6324.
(25) Zhong, M.; Jang, M. Dynamic light absorption of biomass-burning organic carbon photochemically aged under natural sunlight. *Atmos. Chem. Phys.* **2014**, *14*, 1517−1525.
(26) Saleh, R.; Hennigan, C. J.; McMeeking, G. R.; Chuang, W. K.; Robinson, E. S.; Coe, H. M.; Donahue, N. M.; Robinson, A. L. Absorptivity of brown carbon in fresh and photo-chemically aged biomass-burning emissions. *Atmos. Chem. Phys.* **2013**, *13*, 7683−7693.
(27) Lambe, A. T.; Cappa, C. D.; Massoli, P.; Onasch, T. B.; Forestieri, S. D.; Martin, A. T.; Cummings, M. J.; Croasdale, D. R.; Brune, W. H.; Worsnop, D. R.; Davidovits, P. Relationship between Oxidation Level and Optical Properties of Secondary Organic Aerosol. *Environ. Sci. Technol.* **2013**, *47* (12), 6349−6357.
(28) Kang, E.; Root, M. J.; Toohey, D. W.; Brune, W. H. Introducing the concept of Potential Aerosol Mass (PAM). *Atmos. Chem. Phys.* **2007**, *7*, 5727−5744.
(29) Lambe, A. T.; Ahern, A. T.; Williams, L. R.; Slowik, J. G.; Wong, J. P. S.; Abbatt, J. P. D.; Brune, W. H.; Ng, N. L.; Wright, J. P.; Croasdale, D. R.; Worsnop, D. R.; Davidovits, P.; Onasch, T. B. Characterization of aerosol photooxidation flow reactors: heterogeneous oxidation, secondary organic aerosol formation and cloud condensation nuclei activity measurements. *Atmos. Meas. Tech.* **2011**, *4*, 445−461.
(30) Li, R.; Palm, B. B.; Ortega, A. M.; Hlywiak, J.; Hu, W.; Peng, Z.; Day, D. A.; Knote, C.; Brune, W. H.; de Gouw, J. A.; Jimenez, J. L. Modeling the Radical Chemistry in a Oxidation Flow Reactor: Radical Formation and Recycling, Sensitivities, and the OH Exposure Estimation Equation. *J. Phys. Chem. A* **2015**, *119* (19), 4418−4432.
(31) Bruns, E. A.; El Haddad, I.; Keller, A.; Klein, F.; Kumar, N. K.; Pieber, S. M.; Corbin, J. C.; Slowik, J. G.; Brune, W. H.; Baltensperger, U.; Prévôt, A. S. H. Inter-comparison of laboratory smog chamber and flow reactor systems on organic aerosol yield and composition. *Atmos. Meas. Tech.* **2015**, *8*, 2315−2332.
(32) Drinovec, L.; Močnik, G.; Zotter, P.; Prévôt, A. S. H.; Ruckstuhl, C.; Coz, E.; Rupakheti, M.; Sciare, J.; Müller, T.; Wiedensohler, A.; Hansen, A. D. A. *Atmos. Meas. Technol. Disc.* **2014**, *7*, 10179−10220.
(33) Weingartner, E.; Saathoff, H.; Schnaiter, M.; Streit, N.; Bitnar, B.; Baltensperger, U. Absorption of light by soot particles: determination of the absorption coefficient by means of aethalometers. *J. Aerosol Sci.* **2003**, *34* (10), 1445−1463.
(34) Bergstrom, R. W.; Russell, P. B.; Hignett, P. Wavelength Dependence of the Absorption of Black Carbon Patricles: Predictions and Results from the TARFOX Experiment and Implications for the Aerosol Single Scattering Albedo. *J. Atmos. Sci.* **2002**, *59*, 567−577.
(35) Sandradewi, J.; Prévôt, A. S. H.; Szidat, S.; Perron, N.; Alfarra, M. R.; Lanz, V. A.; Weingartner, E.; Baltensperger, U. Using Aerosol Light Absorption Measurements of the Quantitative Determination of Wood Burning and Traffic Emission Contributions to Particulate Matter. *Environ. Sci. Technol.* **2008**, *42* (9), 3316−3323.
(36) Kirchstetter, T. W.; Thatcher, T. L. Contribution of organic carbon to wood smoke particulate matter absorption of solar radiation. *Atmos. Chem. Phys.* **2012**, *12*, 6067−6072.
(37) Onasch, T. B.; Trimborn, A.; Fortner, E. C.; Jayne, J. T.; Kok, G. L.; Williams, L. R.; Davidovits, P.; Worsnop, D. R. Soot Particle Aerosol Mass Spectrometer: Development, Validation, and Initial Application. *Aerosol Sci. Technol.* **2012**, *46* (7), 804−817.
(38) Van Loo, S.; Koppejan, J. *the Handbook of Biomass Combustion and Co-Firing*; Earthscan: London, U.K., 2012.
(39) Willis, M. D.; Lee, A. K. Y.; Onasch, T. B.; Fortner, E. C.; Williams, L. R.; Lambe, A. T.; Worsnop, D. R.; Abbatt, J. P. D. Collection efficiency of the soot-particle aerosol mass spectrometer (SP-AMS) for internally mixed particulate black carbon. *Atmos. Meas. Tech.* **2014**, *7*, 4507−4516.
(40) Bruns, E. A.; Krapf, M.; Orasche, J.; Huang, Y.; Zimmermann, R.; Drinovec, L.; Močnik, G.; El-Haddad, I.; Slowik, J. G.; Dommen, J.; Baltensperger, U.; Prévôt, A. S. H. Characterization of primary and

DOI: 10.1021/acs.est.5b03205
Environ. Sci. Technol. 2015, 49, 14663−14671

secondary wood combustion products generated under different burner loads. *Atmos. Chem. Phys.* **2015**, *15*, 2825−2841.
(41) Hennigan, C. J.; Miracolo, M. A.; Engelhart, G. J.; May, A. A.; Presto, A. A.; Lee, T.; Sullivan, A. P.; McMeeking, G. R.; Coe, H.; Wold, C. E.; Hao, W.-M.; Gilman, J. B.; Kuster, W. C.; de Gouw, J.; Schichtel, B. A.; Collett, J. L., Jr; Kreidenweis, S. M.; Robinson, A. L. Chemical and physical transformations of organic aerosol from the photo-oxidation of open biomass burning emissions in an environmental chamber. *Atmos. Chem. Phys.* **2011**, *11*, 7669−7686.
(42) Schwarz, J. P.; Spackman, J. R.; Fahey, D. W.; Gao, R. S.; Lohmann, U.; Stier, P.; Watts, L. A.; Thomson, D. S.; Lack, D. A.; Pfister, L.; Mahoney, M. J.; Baumgardner, D.; Wilson, J. C.; Reeves, J. M. Coatings and their enhancement of black carbon light absorption on the tropical atmosphere. *J. Geophys. Res.* **2008**, *113* (D3), D03203.
(43) Bond, T. C.; Habib, G.; Bergstrom, R. W. Limitations in the enhancement of visible light absorption due to mixing state. *J. Geophys. Res.* **2006**, *111* (D20),10.1029/2006JD007315

DOI: 10.1021/acs.est.5b03205
Environ. Sci. Technol. 2015, 49, 14663−14671